
Information-Theoretic Privacy Control for Sequential Multi-Agent LLM Systems

Sadia Asif¹ Mohammad Mohammadi Amiri¹

Abstract

Sequential multi-agent large language model (LLM) systems are increasingly deployed in sensitive domains such as healthcare, finance, and enterprise decision-making, where multiple specialized agents collaboratively process a single user request. Although individual agents may satisfy local privacy constraints, sensitive information can still be inferred through sequential composition and intermediate representations. In this work, we study *compositional privacy leakage* in sequential LLM agent pipelines. We formalize leakage using mutual information and derive a theoretical bound that characterizes how locally introduced leakage can amplify across agents under sequential execution. Motivated by this analysis, we propose a privacy-regularized training framework that directly constrains information flow between agent outputs and agent-local sensitive variables. We evaluate our approach across sequential agent pipelines of varying depth on three benchmark datasets, demonstrating stable optimization dynamics and consistent, interpretable privacy-utility trade-offs. Our results show that privacy in agentic LLM systems cannot be guaranteed by local constraints alone and must instead be treated as a system-level property during both training and deployment.

1. Introduction

Large language models (LLMs) are increasingly deployed as *agentic systems*, where complex user requests are handled not by a single monolithic model, but by multiple interacting agents with specialized roles. Such multi-agent architectures enable modular reasoning, tool use, delegation, and specialization, and are now widely adopted in applications

¹Department of Computer Science, Rensselaer Polytechnic Institute, Troy New York. Correspondence to: Sadia Asif <asifs@rpi.edu>, Mohammad Mohammadi Amiri <mamiri@rpi.edu>.

spanning medical decision support, financial analysis, and enterprise automation (Pan et al., 2025; Xiao et al., 2024; Marreed et al., 2025).

In such multi-agent systems, agents can interact in several structural modes, including *parallel* collaboration (agents operating independently and aggregating results), *hierarchical* orchestration (controllers delegating subtasks to workers), and *sequential* pipelines, where agents process information stage-by-stage and pass intermediate representations downstream. Each interaction pattern induces distinct failure modes and security risks. In this work, we focus specifically on *sequential multi-agent pipelines*, a common deployment pattern in real-world systems where intermediate reasoning states, summaries, or tool outputs produced by one agent serve as input to the next.

Despite their practical advantages, sequential agent pipelines introduce *privacy risks* that are not captured by traditional single-model threat models. In realistic deployments, individual agents often operate with *agent-local sensitive context*, such as proprietary policies, internal routing logic, private memory states, or domain-specific confidential data. Although downstream agents may not be granted direct access to this sensitive information, intermediate messages and learned representations can retain statistical dependencies that allow sensitive attributes to be inferred through composition. Consequently, even when each agent individually satisfies a local privacy constraint, the system as a whole may exhibit substantial privacy leakage due to sequential execution.

Prior research on privacy in LLMs has primarily focused on *single-model* settings, including memorization of training data (Xu et al., 2025; Nasr et al., 2025), membership inference attacks (Meeus et al., 2025; Mangaokar et al., 2025), and differential privacy during training (Kulynych et al., 2025). While these approaches provide important guarantees at the model level, they do not address privacy risks that arise *at deployment time* from interactions among multiple agents. More recent work on multi-agent LLM security has examined adversarial prompt propagation, trust miscalibration, and coordination failures (Patil et al., 2025; Zhang et al., 2025; Yang et al., 2025; Gomaa et al., 2025). However, privacy leakage induced by *sequential composi-*

tion of agent representations remains poorly understood and largely unquantified. This gap is increasingly problematic as modern LLM deployments shift toward agentic architectures, where intermediate representations, summaries, and tool outputs are explicitly reused across multiple stages. In such systems, privacy risk no longer stems solely from what a single agent reveals, but from how information is *propagated, transformed, and amplified* across agent boundaries.

Existing privacy techniques are ill-suited to capture this phenomenon. Model-level guarantees (e.g., memorization bounds or differential privacy) treat agents in isolation, while heuristic defenses such as sanitization or access control reason only about surface-level disclosures. Neither perspective accounts for *latent statistical dependencies* embedded in intermediate representations, nor for the cumulative effect of downstream processing. As a result, systems may satisfy strong local privacy constraints at each agent, yet still exhibit substantial *global leakage* once outputs are composed sequentially. Addressing this challenge requires a framework that (i) quantifies privacy at the level of intermediate representations rather than final outputs, and (ii) provides compositional guarantees that scale with pipeline depth. In this paper, we are addressing this gap by using *information-theoretic perspective* to study privacy leakage in sequential LLM agent pipelines.

Contributions. Our main contributions are summarized as follows:

- We formalize *compositional privacy leakage* in sequential multi-agent LLM systems and show that local per-agent privacy constraints are insufficient to guarantee global privacy.
- We derive a theoretical bound characterizing how information leakage amplifies across sequential agent pipelines under standard Markov assumptions.
- We propose a privacy-regularized training framework that directly constrains mutual information (MI) between intermediate agent representations and agent-local sensitive variables.
- We provide extensive empirical evaluation across medical, financial, and action-based privacy benchmarks, demonstrating consistent and interpretable privacy-utility trade-offs.

2. Related Work

A large body of work has studied privacy risks in LLMs, primarily focusing on memorization-based attacks and training-data leakage. Prior studies demonstrate that LLMs can regurgitate sensitive sequences from their training data through extraction and membership inference attacks (Shokri et al., 2017; Carlini et al., 2022; Ippolito et al., 2023), with memorization scaling with model size and data repetition. More recent work has expanded this scope to inference-time pri-

vacuity violations, where models infer sensitive attributes from prompts or contextual cues even when such information was not explicitly memorized (Staab et al., 2024; Wu et al., 2025). While effective at characterizing single-model risks, these approaches largely assume centralized interaction and do not account for privacy leakage emerging from multi-step or distributed reasoning.

In parallel, research on contextual privacy emphasizes that privacy is not an absolute property but depends on socially appropriate information flows (Bagdasarian et al., 2024). Benchmarks such as PrivacyLens operationalize this view by evaluating whether model actions violate contextual integrity under realistic scenarios (Shao et al., 2024). However, these approaches evaluate privacy primarily at the level of final actions or decisions, leaving open how intermediate representations contribute to downstream leakage when composed across multiple agents.

The rise of multi-agent LLM systems further complicates this landscape (Zhang & Yang, 2025). Agentic frameworks decompose complex tasks into sequences of specialized agents, often sharing intermediate representations, tool outputs, or memory states (Talebirad & Nadiri, 2023; Khan & Asif, 2025; Prabhakar et al., 2025). Although such decomposition improves task performance, recent studies reveal that agent communication and memory mechanisms introduce new attack surfaces, including memory poisoning and cross-agent inference (Gomaa et al., 2025; Rosser & Foerster, 2025). Existing defenses focus on sanitization, prompt filtering, or architectural isolation, but lack principled guarantees against leakage arising from sequential composition. Our work differs from prior literature in two key respects. First, we study privacy leakage as a *compositional phenomenon*, showing that even benign, locally safe agent outputs can jointly reveal sensitive attributes when aggregated. Second, we provide an information-theoretic framework that quantifies this leakage at the representation level and yields formal guarantees on cumulative risk. A more detailed discussion of memorization attacks, contextual integrity, agent memory vulnerabilities, and their limitations is provided in Appendix A.6.

3. Problem Setup

We now formalize privacy leakage in sequential multi-agent LLM systems from an information-theoretic perspective. Our focus is on understanding how sensitive information held locally by individual agents propagates through intermediate representations and accumulates under sequential composition. We begin by introducing the system model and threat assumptions, then define a notion of compositional privacy leakage that captures system-level exposure arising from multi-agent execution. This formulation provides the foundation for our theoretical analysis of leakage amplification and motivates the privacy-regularized training framework developed in subsequent sections.

3.1. Sequential Agent Pipeline

We consider a sequential multi-agent system in which a single user request is processed through a pipeline of N specialized agents, $\{a_1, \dots, a_N\}$. The request is first handled by agent a_1 , whose output is passed to a_2 , and so on, until agent a_N produces the final system response.

Let $O_0 \triangleq \emptyset$ denote an empty initial input. For each agent a_i , we define:

- D_i as public or task-relevant inputs to agent a_i ,
- S_i as *agent-local sensitive information* accessible only to agent a_i and $S_{<i} = \{S_1, \dots, S_{i-1}\}$,
- O_i as the output representation produced by agent a_i .

Agent execution follows the sequential update rule

$$O_i = A_i(O_{i-1}, D_i, S_i), \quad i = 1, \dots, N, \quad (1)$$

where O_{i-1} denotes the output received from the preceding agent. The final system output is given by O_N .

Conditional Independence Structure. We assume that each agent’s output depends on its local sensitive context only through its own computation, and that downstream agents do not access upstream sensitive variables directly. Formally, the sequential pipeline satisfies the conditional Markov structure

$$S_{i-1} \rightarrow (O_{i-1}, D_i, S_i) \rightarrow O_i \rightarrow O_{i+1} \rightarrow \dots \rightarrow O_N, \quad (2)$$

for each $i \in \{1, \dots, N\}$.

Interpretation. Eq. (2) formalizes the assumption that sensitive information introduced at earlier stages influences downstream behavior only through the intermediate representations that are explicitly passed along the pipeline. Conditioned on the information available to agent a_i —namely the upstream output O_{i-1} , task-relevant inputs D_i , and its own local sensitive context S_i —the agent’s output O_i is independent of upstream sensitive variables S_{i-1} . As a result, any leakage of upstream sensitive information into later outputs must occur indirectly via sequential transformation and reuse of intermediate representations, rather than through direct access to private agent state. Although S_i is never explicitly transmitted, statistical dependencies between S_i and the agent’s output O_i can induce privacy leakage. Because intermediate outputs are reused by downstream agents, such leakage may propagate and accumulate through the pipeline via sequential transformations.

To quantify this phenomenon, we adopt an information-theoretic perspective and measure privacy leakage using MI. We define the *global compositional leakage* as

$$\mathcal{L}_{\text{global}} \triangleq I(O_N; S_1, \dots, S_N), \quad (3)$$

which captures how much information about all agent-local sensitive variables $\{S_i\}_{i=1}^N$ can be inferred from the final

system output O_N . This definition naturally accounts for indirect leakage arising from sequential composition, even when no individual agent directly discloses its sensitive context.

3.2. Threat Model

We assume an adversary that observes the final output O_N and seeks to infer information about the sensitive variables $\{S_i\}_{i=1}^N$. The adversary does not have direct access to agent internals, intermediate representations, or private contexts, but can exploit statistical correlations induced by sequential execution and representation passing.

This threat model captures both external observers accessing system outputs and internal agents attempting to infer upstream sensitive information from shared representations.

3.3. Privacy Objective

Our objective is to design learning and execution mechanisms that limit compositional privacy leakage while preserving task utility. Formally, we aim to control the global leakage $\mathcal{L}_{\text{global}}$ subject to maintaining performance on the target task.

Achieving this objective requires understanding how privacy loss arises from the interaction of agents through shared intermediate representations, rather than from any single agent in isolation. In the next section, we formally analyze how privacy leakage behaves under sequential composition and characterize the fundamental limits of agent-local privacy control.

4. Theoretical Analysis for Compositional Privacy Leakage

We now provide a formal analysis of privacy leakage in sequential multi-agent systems. Our goal is to characterize how information about agent-local sensitive variables propagates through intermediate representations and accumulates at the system output.

We show that even when each agent individually satisfies a bounded local privacy constraint, the sequential reuse and transformation of representations can induce significantly larger leakage at the system level. This theoretical analysis reveals a fundamental gap between agent-local privacy guarantees and end-to-end privacy behavior in composed agent pipelines.

4.1. Per-Agent Leakage

For each agent a_i , we quantify *local leakage* as the MI between the agent’s output representation O_i and its agent-local sensitive variable S_i :

$$I(O_i; S_i). \quad (4)$$

A natural design goal is to enforce a per-agent privacy constraint of the form

$$I(O_i; S_i) \leq \epsilon_i, \quad (5)$$

where $\epsilon_i \geq 0$ denotes a user-specified privacy budget for agent a_i .

Such constraints ensure that no single agent output reveals excessive information about its own sensitive context. However, as we show next, local control alone is insufficient to bound the privacy risk of the composed system.

4.2. Sequential Composition and Leakage Amplification

Our analysis focuses on how the global compositional leakage defined in Eq. (3) evolves under sequential execution. Although each agent may satisfy a local information constraint, dependencies introduced at early stages are repeatedly transformed by downstream agents, leading to amplified exposure at the final output. We show that this accumulation effect can dominate system-level behavior, rendering agent-local guarantees insufficient in deep pipelines.

Local vs. Global Leakage. While per-agent leakage bounds defined in Eq. (5) control direct disclosure at individual stages, they do not characterize how information propagates across the pipeline. In sequential settings, correlations introduced upstream are transformed and reused by downstream agents, allowing sensitive dependence to accumulate beyond what any single agent reveals in isolation. As a result, system-level privacy behavior can differ qualitatively from agent-level guarantees.

Theorem 4.1 (Cumulative Leakage Bound). *Consider a sequential agent pipeline satisfying the Markov structure as given in Eq. (2) and assume that the sensitive variables $\{S_i\}_{i=1}^N$ are mutually independent. If each agent satisfies the local leakage constraint $I(O_i; S_i) \leq \epsilon_i$, then the global compositional leakage satisfies*

$$I(O_N; S_1, \dots, S_N) \leq \sum_{i=1}^N 2^{N-i} \epsilon_i. \quad (6)$$

Interpretation. Theorem 4.1 (proof given in Appendix A.1) reveals an inherent *amplification effect* under sequential composition: leakage introduced by earlier agents is repeatedly transformed and propagated by downstream agents, resulting in an exponentially growing contribution to the final output. In the uniform case $\epsilon_i = \epsilon$, the bound reduces to $(2^N - 1)\epsilon$, indicating that even modest per-agent leakage can yield substantial global exposure as the pipeline depth increases. Although this result is stated as an upper bound, our experimental results in Section 7.3 empirically exhibit the same depth-dependent amplification trend, confirming that the bound captures a practically relevant failure mode rather than a purely vacuous worst case.

Early-Agent Dominance. The structure of the bound implies that leakage introduced by earlier agents contributes exponentially more to the final leakage than leakage introduced by later agents. This asymmetry motivates stronger

privacy control at early stages of the pipeline and is empirically validated in our ablation studies provided in Appendix A.5.

Proposition 4.2 (Early-Agent Leakage Dominance). *For fixed $\{\epsilon_i\}_{i=1}^N$, the marginal contribution of ϵ_i to $I(O_N; S_1, \dots, S_N)$ scales as 2^{N-i} , implying that leakage at earlier agents dominates global compositional leakage.*

4.3. Design Implications

Theorem 4.1 demonstrates that enforcing independent, per-agent privacy constraints does not suffice to control privacy risk in sequential pipelines. Instead, privacy must be treated as a system-level property that explicitly accounts for downstream amplification effects. This observation motivates learning objectives that directly regulate information flow throughout the pipeline, rather than relying on post hoc filtering or isolated local defenses.

In the next section, we introduce a privacy-regularized training framework that operationalizes this principle by explicitly penalizing MI between agent outputs and agent-local sensitive variables during training.

5. Privacy-Regularized Sequential Agent Training

We now describe a training framework that explicitly controls privacy leakage in sequential multi-agent systems. Motivated by the theoretical analysis of compositional privacy leakage in Section 4.1, our approach introduces an information-theoretic regularization term that constrains the dependence between each agent’s output and its agent-local sensitive context during training.

5.1. Training Objective

Our objective is to preserve task utility while limiting information leakage at each stage of the agent pipeline. Let y denote the ground-truth task label. The final agent output O_N is used to compute a standard supervised utility loss

$$\mathcal{L}_{\text{utility}} = \ell(O_N, y), \quad (7)$$

where $\ell(\cdot)$ denotes a standard task loss (e.g., cross-entropy). To control privacy leakage, we penalize the MI between each agent’s output and its corresponding sensitive variable:

$$\mathcal{L}_{\text{privacy}} = \sum_{i=1}^N \beta_i I(O_i; S_i), \quad (8)$$

where $\beta_i \geq 0$ determines the privacy-utility trade-off at agent a_i . The resulting optimization problem is

$$\mathcal{L}_{\text{total}} = \mathcal{L}_{\text{utility}} + \mathcal{L}_{\text{privacy}}. \quad (9)$$

5.2. Mutual Information Estimation

Direct computation of the MI $I(O_i; S_i)$ is intractable for high-dimensional neural representations produced by large

language models. We therefore adopt a variational estimation approach based on the Donsker–Varadhan (DV) representation of the Kullback–Leibler (KL) divergence, as instantiated by Mutual Information Neural Estimation (MINE) (Belghazi et al., 2018).

Donsker–Varadhan Representation. For two distributions P and Q defined on a common support Ω , the KL-divergence admits the variational form

$$D_{\text{KL}}(P \parallel Q) = \sup_{T: \Omega \times \Omega \rightarrow \mathbb{R}} \{ \mathbb{E}_P[T] - \log \mathbb{E}_Q[e^T] \}, \quad (10)$$

where the supremum is taken over all measurable functions T for which the expectations are finite.

By setting $P = p(o_i, s_i)$ and $Q = p(o_i)p(s_i)$, the MI between an agent’s output O_i and its sensitive variable S_i can be written as

$$\begin{aligned} I(O_i; S_i) &= D_{\text{KL}}(p(o_i, s_i) \parallel p(o_i)p(s_i)) \\ &= \sup_{T \in \mathcal{F}} \left\{ \mathbb{E}_{p(o_i, s_i)}[T(o_i, s_i)] \right. \\ &\quad \left. - \log \mathbb{E}_{p(o_i)p(s_i)}[e^{T(o_i, s_i)}] \right\}, \quad (11) \end{aligned}$$

where \mathcal{F} denotes a parameterized function family.

Neural Estimator Formulation. In practice, we restrict \mathcal{F} to a family of neural networks $T_{\psi_i} : \mathcal{O}_i \times \mathcal{S}_i \rightarrow \mathbb{R}$, where \mathcal{O}_i denotes the intermediate representation produced by agent a_i and \mathcal{S}_i denotes the corresponding agent-local sensitive variable, referred to as *critics*, with parameters ψ_i . Given a minibatch of size B , we obtain empirical joint samples $\{(o_i^{(b)}, s_i^{(b)})\}_{b=1}^B$ from $p(o_i, s_i)$, and approximate samples from the product of marginals $p(o_i)p(s_i)$ by pairing $o_i^{(b)}$ with shuffled sensitive variables $s_i'^{(b)}$ within the minibatch.

The resulting sample-based MINE estimator is

$$\begin{aligned} \hat{I}_{\text{MINE}}(O_i; S_i) &= \frac{1}{B} \sum_{b=1}^B T_{\psi_i}(o_i^{(b)}, s_i^{(b)}) \\ &\quad - \log \left(\frac{1}{B} \sum_{b=1}^B \exp(T_{\psi_i}(o_i^{(b)}, s_i'^{(b)})) \right). \quad (12) \end{aligned}$$

This estimator provides a differentiable bound on the true mutual information and serves as a quantitative measure of privacy leakage at agent a_i .

Optimization and Stability. During training, the critic parameters ψ_i are updated to *maximize* $\hat{I}_{\text{MINE}}(O_i; S_i)$ in Eq. (12), while the agent parameters are updated to *minimize* the same quantity as part of the overall privacy-regularized

objective. To improve numerical stability of the logarithmic partition term, we maintain an exponential moving average of $\exp(T_{\psi_i})$, following standard and empirically validated MINE implementations (Belghazi et al., 2018).

5.3. Optimization Procedure

Training proceeds iteratively and alternates between estimating mutual information and updating the agent parameters to minimize $\mathcal{L}_{\text{total}}$ given in Eq. (9). Each iteration consists of three phases: (i) a forward pass through the agent pipeline to obtain $\mathcal{L}_{\text{utility}}$, (ii) updating the MINE critics to obtain accurate estimates of $\hat{I}_{\text{MINE}}(O_i; S_i)$, and (iii) updating the agent parameters by minimizing the combined objective $\mathcal{L}_{\text{total}}$, which balances task utility and privacy regularization. The complete training procedure is summarized in Algorithm 1.

Algorithm 1 Information-Regularized Multi-Agent Training with MINE

- 1: Initialize agent parameters $\{\theta_i\}_{i=1}^N$ and estimator parameters $\{\psi_i\}_{i=1}^N$.
 - 2: **for** iteration $t = 1$ to T **do**
 - 3: **Phase 1: Forward Pass**
 - 4: Compute sequential outputs: $O_1 \rightarrow O_2 \rightarrow \dots \rightarrow O_N$.
 - 5: Compute utility loss: $\mathcal{L}_{\text{utility}} = \ell(O_N, y)$.
 - 6: **Phase 2: MINE Estimator Update**
 - 7: **for** each agent a_i **do**
 - 8: Sample joint pairs $(o_i, s_i) \sim p(o_i, s_i)$.
 - 9: Sample marginal pairs (o_i, s_i') by shuffling S_i .
 - 10: Estimate $\hat{I}_{\text{MINE}}(O_i; S_i)$ using Eq. (12).
 - 11: Update $\psi_i \leftarrow \psi_i + \eta_{\psi} \nabla_{\psi_i} \hat{I}_{\text{MINE}}(O_i; S_i)$.
 - 12: **end for**
 - 13: **Phase 3: Agent Update**
 - 14: Compute total loss: $\mathcal{L}_{\text{total}} = \mathcal{L}_{\text{utility}} + \sum_i \beta_i \hat{I}_{\text{MINE}}(O_i; S_i)$.
 - 15: Update agent parameters: $\theta_i \leftarrow \theta_i - \eta_{\theta} \nabla_{\theta_i} \mathcal{L}_{\text{total}}$.
 - 16: **end for**
-

This optimization enforces an explicit information bottleneck at each agent boundary. As a result, agents learn representations that are sufficient for task completion while minimizing the propagation of agent-local sensitive context through the sequential pipeline.

6. Experimental Setup

We evaluate our privacy-regularized training framework on sequential multi-agent LLM systems across multiple domains. Our experiments are designed to isolate how privacy leakage and task utility scale with agent depth, model capacity, and task domain.

Benchmarks. We consider three privacy-critical benchmarks: *MedQA* (Jin et al., 2020) for medical reasoning, *FinQA* (Chen et al., 2021) for financial numerical reason-

Table 1. MedQA results for LLaMA models (B=Baseline, M=MINE-Reg); Ag = number of agents.

Model	Ag	Meth	CE ↓	MI _{avg} ↓	SB ↑	BS ↑	PI ↑	PARI ↑
LLaMA-7B	2	B	1.32	0.49	0.42	0.95	0.000	0.480
	2	M	1.47	0.06	0.81	0.89	0.878	0.901
	3	B	1.54	0.70	0.33	0.93	0.000	0.474
	3	M	1.68	0.08	0.78	0.87	0.886	0.899
	4	B	1.73	0.90	0.26	0.90	0.000	0.465
	4	M	1.92	0.10	0.74	0.84	0.889	0.891
	5	B	1.88	1.05	0.21	0.87	0.000	0.456
5	M	2.06	0.14	0.70	0.81	0.867	0.871	
LLaMA-3B	2	B	1.55	0.62	0.34	0.86	0.000	0.453
	2	M	1.72	0.18	0.66	0.78	0.710	0.784
	3	B	1.71	0.80	0.29	0.83	0.000	0.444
	3	M	1.89	0.22	0.62	0.77	0.725	0.788
	4	B	1.88	0.96	0.25	0.80	0.000	0.435
	4	M	2.05	0.27	0.58	0.74	0.719	0.776
	5	B	2.02	1.12	0.20	0.77	0.000	0.426
5	M	2.21	0.33	0.54	0.71	0.705	0.761	

ing, and *PrivacyLens* (Shao et al., 2024) for action-based evaluation of contextual privacy norms. Together, these benchmarks cover classification-style reasoning, numerical program execution, and realistic agent trajectories where privacy violations may emerge only through sequential composition.

Sequential Agent Pipelines. We evaluate pipelines of $N \in \{2, 3, 4, 5\}$ agents executed sequentially. Each agent is an independent LLM that communicates exclusively via intermediate representations, reflecting common real-world deployments where reasoning, planning, and policy enforcement are handled by distinct components.

Models. Experiments are conducted using open-weight LLMs from the Qwen (2B, 4B) and LLaMA (3B, 7B) families,¹ fine-tuned with LoRA adapters (Hu et al., 2021). Agents do not share parameters unless explicitly stated.

Training and Baselines. We compare standard end-to-end training against privacy-regularized training that penalizes MI between intermediate agent representations and agent-local sensitive variables. Details of the objective and sensitive variable definitions are provided in Appendix A.2.

Evaluation. Utility is measured using task-appropriate accuracy or helpfulness metrics, while privacy is evaluated using MI estimates, adversarial leakage accuracy, and composite privacy-utility scores. Formal metric definitions are given in Appendix A.3.

¹Qwen models: <https://huggingface.co/Qwen/Qwen2-1.5B>, <https://huggingface.co/Qwen/Qwen1.5-4B-Chat>. LLaMA models: <https://huggingface.co/meta-llama/Llama-3.2-3B>, <https://huggingface.co/meta-llama/Llama-2-7b>.

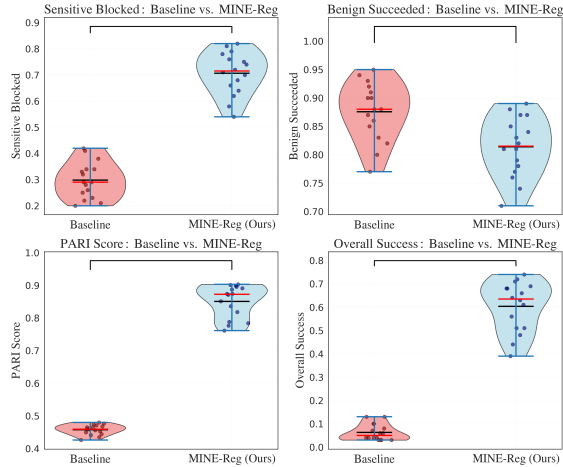


Figure 1. Distributional comparison of baseline and MINE-Reg across privacy and utility metrics for LLaMA-3B. Violin plots show per-run variability with mean (red bar) and dispersion for Sensitive Blocked, Benign Succeeded, PARI score, and Overall Success.

7. Results

In this section, we provide the results of our proposed information-theoretic regularization framework on **medical** (MedQA) (Jin et al., 2020) and **financial** (FinQA) (Chen et al., 2021) reasoning benchmarks, focusing on privacy leakage, task utility, and their interaction under sequential multi-agent composition. All metrics follow the formal definitions given in Appendix A.3. Results on the PrivacyLens (Shao et al., 2024) benchmark are deferred to Appendix A.4.

7.1. Overall Performance on Medical and Financial Benchmarks

Tables 1, 2 report MedQA results, while Tables 3, 4 report FinQA results. Across both domains and all agent depths (2–5 agents), MI-regularized training (MINE-Reg) consistently reduces compositional leakage and improves system-level privacy outcomes, while preserving the majority of benign task performance. Two consistent patterns emerge from the tables: (i) unregularized baselines exhibit progressively worse privacy with increasing depth, and (ii) MINE-Reg flattens this depth-induced degradation, yielding substantially higher privacy protection at comparable utility.

MINE-Reg achieves large reductions in MI_{avg} relative to the baseline, typically in the **75–90%** range depending on depth and model scale. On the MedQA benchmark, for Qwen-4B with two agents, MI_{avg} drops from 0.54 to 0.06 ($\approx 89\%$ reduction), and remains low even as the pipeline deepens (e.g., 0.13 at five agents versus a baseline of 1.02). Similarly on the FinQA benchmark, LLaMA-7B reduces MI_{avg} from 0.51 to 0.06 at two agents ($\approx 88\%$), and from 1.10 to 0.15 at five agents ($\approx 86\%$). These reductions translate into consistent gains in adversarial failure rates: Sensitive Blocked (SB) increases by roughly **+0.35 to +0.50** across

Table 2. MedQA results for Qwen models (B=Baseline, M=MINE-Reg); Ag = number of agents.

Model	Ag	Meth	CE ↓	MI _{avg} ↓	SB ↑	BS ↑	PI ↑	PARI ↑	
Qwen-4B	2	B	1.40	0.54	0.38	0.94	0.000	0.477	
	2	M	1.58	0.06	0.82	0.88	0.889	0.903	
	3	B	1.62	0.73	0.32	0.92	0.000	0.471	
	3	M	1.77	0.08	0.79	0.85	0.890	0.895	
	4	B	1.75	0.88	0.28	0.90	0.000	0.465	
	4	M	1.93	0.10	0.75	0.83	0.886	0.887	
	5	B	1.89	1.02	0.22	0.88	0.000	0.459	
	5	M	2.05	0.13	0.71	0.81	0.873	0.874	
	Qwen-2B	2	B	1.48	0.61	0.41	0.91	0.000	0.468
		2	M	1.55	0.10	0.76	0.87	0.836	0.874
3		B	1.66	0.78	0.34	0.88	0.000	0.459	
3		M	1.74	0.14	0.72	0.82	0.821	0.851	
4		B	1.82	0.94	0.29	0.85	0.000	0.450	
4		M	1.93	0.18	0.68	0.79	0.809	0.836	
5		B	1.98	1.10	0.23	0.82	0.000	0.441	
5		M	2.10	0.23	0.64	0.76	0.791	0.818	

Table 3. FinQA results for LLaMA models (B=Baseline, M=MINE-Reg); Ag = number of agents.

Model	Ag	Meth	CE ↓	MI _{avg} ↓	SB ↑	BS ↑	PI ↑	PARI ↑	
LLaMA-7B	2	B	1.38	0.51	0.40	0.94	0.000	0.481	
	2	M	1.53	0.06	0.82	0.88	0.882	0.905	
	3	B	1.61	0.72	0.31	0.90	0.000	0.472	
	3	M	1.78	0.09	0.77	0.84	0.875	0.890	
	4	B	1.79	0.93	0.25	0.89	0.000	0.466	
	4	M	1.98	0.11	0.73	0.83	0.882	0.892	
	5	B	1.95	1.10	0.20	0.86	0.000	0.458	
	5	M	2.14	0.15	0.69	0.80	0.864	0.872	
	LLaMA-3B	2	B	1.62	0.69	0.31	0.85	0.000	0.449
		2	M	1.78	0.21	0.69	0.77	0.696	0.778
3		B	1.79	0.87	0.26	0.82	0.000	0.441	
3		M	1.96	0.26	0.64	0.75	0.701	0.781	
4		B	1.95	1.02	0.22	0.79	0.000	0.433	
4		M	2.13	0.31	0.60	0.72	0.696	0.768	
5		B	2.10	1.18	0.18	0.76	0.000	0.425	
5		M	2.28	0.37	0.56	0.69	0.686	0.755	

most configurations. For example, on MedQA with Qwen-4B, SB improves from 0.38 → 0.82 at two agents and from 0.22 → 0.71 at five agents; on FinQA with LLaMA-7B, SB improves from 0.40 → 0.82 at two agents and from 0.20 → 0.69 at five agents. Notably, the privacy integrity (PI) component mirrors these trends, rising from 0 for baselines (by definition) to ≈ 0.69–0.89 under MINE-Reg, indicating substantial suppression of sensitive dependence.

Utility Preservation. Despite strong privacy improvements, benign accuracy remains comparatively stable under regularization. Across MedQA, Benign Succeeded (BS) typically decreases by **6–8 points** for larger models (e.g., Qwen-4B: 0.94 → 0.88 at two agents; LLaMA-7B: 0.95 → 0.89), and by **8–10 points** for smaller models (e.g., LLaMA-3B: 0.86 → 0.78). On FinQA, benign success is similarly preserved, with LLaMA-7B decreasing from 0.94 → 0.88 at two agents and 0.86 → 0.80 at five agents. Cross-entropy (CE) increases modestly under MINE-Reg (reflecting the expected privacy-utility trade-off), but the degradation remains bounded and does not eliminate the gains in system-level reliability.

Table 4. FinQA results for Qwen models (B=Baseline, M=MINE-Reg); Ag = number of agents.

Model	Ag	Meth	CE ↓	MI _{avg} ↓	SB ↑	BS ↑	PI ↑	PARI ↑	
Qwen-4B	2	B	1.46	0.57	0.36	0.93	0.000	0.479	
	2	M	1.63	0.07	0.80	0.87	0.877	0.900	
	3	B	1.69	0.75	0.31	0.91	0.000	0.473	
	3	M	1.84	0.09	0.77	0.84	0.880	0.892	
	4	B	1.82	0.92	0.27	0.88	0.000	0.464	
	4	M	1.99	0.12	0.73	0.81	0.870	0.878	
	5	B	1.96	1.08	0.21	0.85	0.000	0.455	
	5	M	2.15	0.16	0.69	0.79	0.852	0.863	
	Qwen-2B	2	B	1.54	0.64	0.34	0.90	0.000	0.468
		2	M	1.62	0.12	0.76	0.85	0.812	0.858
3		B	1.71	0.82	0.28	0.87	0.000	0.459	
3		M	1.80	0.16	0.72	0.80	0.805	0.842	
4		B	1.88	0.98	0.24	0.84	0.000	0.451	
4		M	1.98	0.21	0.68	0.77	0.786	0.827	
5		B	2.03	1.15	0.19	0.81	0.000	0.442	
5		M	2.15	0.26	0.64	0.74	0.774	0.812	

Privacy-Aware Reasoning Index (PARI). The composite metric PARI improves substantially across all settings, reflecting simultaneous gains in privacy integrity and preserved reasoning correctness. For Qwen-4B on MedQA, PARI increases from 0.477 → 0.903 at two agents and from 0.459 → 0.874 at five agents; for LLaMA-7B on FinQA, PARI increases from 0.481 → 0.905 at two agents and from 0.458 → 0.872 at five agents. These improvements indicate that MI-regularization yields a consistently better operating point for privacy-sensitive sequential deployments, particularly as agent depth increases.

7.2. Privacy-Utility Trade-off Analysis

Figure 1 provides a distributional comparison between unregularized baselines and MINE-Reg for Llama-3B across varying agent depths on the MedQA benchmark. Rather than emphasizing individual configurations, this analysis highlights system-level trends aggregated across experimental settings.

Privacy Gains. The top-left panel shows the distribution of SB. Baseline systems cluster in the low-privacy regime (SB ≈ 0.20–0.40), indicating widespread vulnerability under sequential composition. In contrast, MINE-Reg shifts the distribution upward, with median SB near 0.70 and upper quartiles exceeding 0.80, demonstrating consistent privacy improvements across models and depths.

Utility Preservation. The top-right panel reports BS. While MINE-Reg introduces a modest utility reduction, performance remains concentrated in the high-accuracy regime (BS ≈ 0.78–0.88). The substantial overlap with baseline distributions confirms that privacy gains are not achieved via catastrophic utility loss, consistent with the 5–9 point BS drops observed in Tables 1, 2, 3 and 4.

Composite System Performance. The bottom-left panel reports the PARI. Baseline systems cluster around 0.44–0.48, reflecting persistent leakage despite strong benign

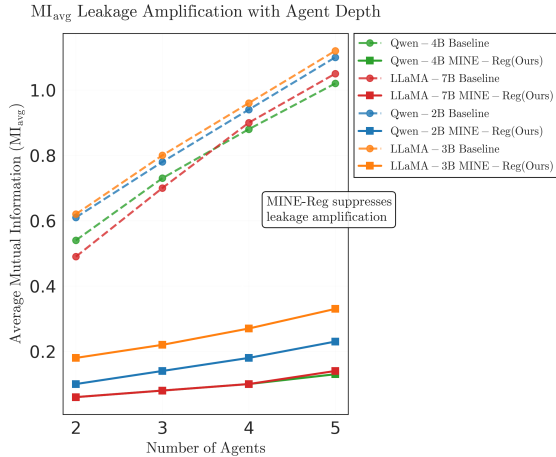


Figure 2. MI_{avg} leakage as a function of sequential agent depth across different models for MedQA benchmark. Unregularized systems exhibit strong leakage amplification with depth, while MI-regularized training effectively suppresses cumulative leakage across all model families.

accuracy. MINE-Reg shifts PARI sharply upward, with medians near 0.87–0.90, indicating a strictly better privacy-utility operating point.

Overall Success (OS). Similarly, the bottom-right panel shows OS, which requires both correct benign behavior and successful privacy protection. Baseline systems fail almost universally ($OS < 0.10$), whereas MINE-Reg concentrates mass between 0.55 and 0.70. This sharp separation indicates that privacy regularization not only mitigates leakage but also enables reliable end-to-end task completion under safety constraints.

7.3. Leakage Amplification with Agent Depth

Figure 2 illustrates how representation-level MI_{avg} evolves with sequential agent depth for Qwen-2B, Qwen-4B, LLaMA-3B, and LLaMA-7B models. Across all model families, unregularized baselines exhibit clear leakage amplification: MI_{avg} increases monotonically as the number of agents grows from two to five, consistent with compounding disclosure effects predicted by Theorem 4.1. For example, on MedQA with LLaMA-7B, MI_{avg} rises from 0.49 at two agents to 1.05 at five agents, with similar trends observed for Qwen variants.

In contrast, MI-regularized training substantially suppresses this amplification across all models. Under MINE-Reg, MI_{avg} remains bounded and grows only mildly with depth, staying below approximately 0.35 even at five agents. This separation between baseline and regularized curves highlights that local per-agent constraints alone are insufficient in deep pipelines, and that explicit system-level MI regularization is necessary to control cumulative privacy leakage under sequential composition.

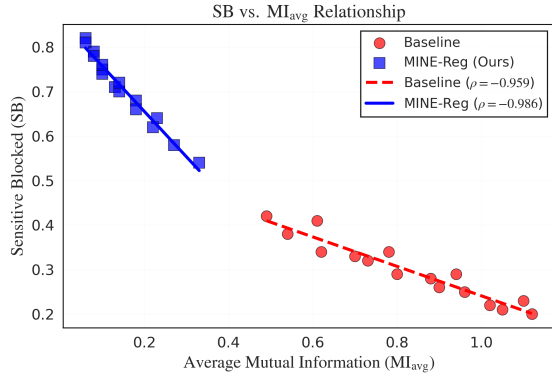


Figure 3. Relationship between MI_{avg} and SB for Qwen-4B model on FinQA benchmark. Strong negative correlations validate the information-theoretic formulation: reducing MI directly improves privacy, with steeper gains under MI-regularized training.

7.4. Information-Theoretic Validation

Figure 3 empirically validates the information-theoretic foundation of our approach by showing a strong negative relationship between MI_{avg} and SB for the Qwen-4B model on the FinQA benchmark. Both unregularized baselines and MINE-Reg exhibit a strong negative correlation between MI_{avg} and SB, with Pearson coefficients of $\rho = -0.959$ and $\rho = -0.986$, respectively. This near-linear dependence confirms that reducing MI_{avg} directly improves privacy outcomes, supporting it as a reliable proxy for leakage risk. Notably, the steeper slope under MI-regularization indicates heightened sensitivity in low-leakage regimes, where small reductions in MI_{avg} yield disproportionately large gains in privacy protection. These findings empirically support the cumulative leakage analysis in Section 4, demonstrating that controlling representation-level MI effectively bounds downstream privacy risk.

8. Conclusion and Future Work

We analyzed privacy leakage in sequential multi-agent LLM pipelines and showed that local privacy guarantees fail to compose, leading to amplified global leakage. To address this, we introduced MI-regularized training (MINE-Reg), a system-level approach that directly constrains information flow at intermediate representations. Both theoretical analysis and experiments on medical and financial benchmarks demonstrate that MINE-Reg effectively suppresses cumulative leakage while preserving task utility, yielding large gains in overall system reliability.

Several directions remain open. Extending the framework to dynamic or adaptive agent pipelines would better reflect real-world deployments. Incorporating leakage-aware orchestration and studying interactions with other privacy mechanisms, such as differential privacy or secure inference, are promising avenues. Finally, applying this approach to larger foundation models and multimodal agent systems

remains an important direction for future work.

References

- Bagdasarian, E., Yi, R., Ghalebikesabi, S., Kairouz, P., Gruteser, M., Oh, S., Balle, B., and Ramage, D. Airgapagent: Protecting privacy-conscious conversational agents. In *Proceedings of the 2024 ACM SIGSAC Conference on Computer and Communications Security (CCS 2024)*, pp. 3868–3882. ACM, 2024.
- Belghazi, M. I., Baratin, A., Rajeswar, S., Ozair, S., Bengio, Y., Courville, A., and Hjelm, R. D. Mutual information neural estimation. In *Proceedings of the 35th International Conference on Machine Learning (ICML 2018)*, volume 80, Stockholm, Sweden, 2018. PMLR.
- Carlini, N., Chien, S., Nasr, M., Song, S., Terzis, A., and Tramèr, F. Membership inference attacks from first principles. In *2022 IEEE Symposium on Security and Privacy (SP)*, pp. 1897–1914. IEEE, 2022.
- Chen, Z., Chen, W., Smiley, C., Shah, S., Borova, I., Langdon, D., Moussa, R., Beane, M., Huang, T.-H., Routledge, B., and Wang, W. Y. Finqa: A dataset of numerical reasoning over financial data. *arXiv preprint arXiv:2109.00122*, 2021. URL <https://arxiv.org/pdf/2109.00122>. Affiliations: University of California, Santa Barbara; J.P. Morgan; Pennsylvania State University; Carnegie Mellon University.
- Chen, Z., Xiang, Z., Xiao, C., Song, D., and Li, B. Agentpoison: Red-teaming llm agents via poisoning memory or knowledge bases. *arXiv preprint arXiv:2407.12784*, 2024. URL <https://arxiv.org/pdf/2407.12784>. Affiliations: University of Chicago; University of Illinois Urbana-Champaign; University of Wisconsin–Madison; University of California, Berkeley.
- Gomaa, A., Salem, A., and Abdelnabi, S. Converse: Benchmarking contextual safety in agent-to-agent conversations. *arXiv preprint arXiv:2511.05359*, 2025. URL <https://arxiv.org/abs/2511.05359>. Affiliations: German Research Center for Artificial Intelligence (DFKI); Microsoft; ELLIS Institute Tübingen and MPI for Intelligent Systems; Tübingen AI Center.
- Hu, E., Shen, Y., Wallis, P., Allen-Zhu, Z., Li, Y., Wang, S., Wang, L., and Chen, W. Lora: Low-rank adaptation of large language models. *arXiv preprint arXiv:2106.09685*, 2021. URL <https://arxiv.org/pdf/2106.09685>. Affiliation: Microsoft Corporation.
- Ippolito, D., Tramèr, F., Nasr, M., Zhang, C., Jagielski, M., Lee, K., Choquette-Choo, C., and Carlini, N. Preventing generation of verbatim memorization in language models gives a false sense of privacy. In *Proceedings of the 16th International Natural Language Generation Conference*, pp. 28–53, 2023.
- Jin, D., Pan, E., Oufattole, N., Weng, W.-H., Fang, H., and Szolovits, P. What disease does this patient have? a large-scale open domain question answering dataset from medical exams. *arXiv preprint arXiv:2009.13081*, 2020. URL <https://arxiv.org/pdf/2009.13081>. Affiliations: MIT, USA; Tongji Medical College, HUST, PRC.
- Khan, H. and Asif, S. Generative ai agents for controllable and protected content creation. In *NeurIPS 2025 Workshop on Generative AI for Provenance, Copyright, and Control (GenProCC)*, 2025. Published: 24 Sept 2025; Last modified: 07 Nov 2025.
- Kulynych, B., Gomez, J. F., Kaissis, G., Hayes, J., Balle, B., Calmon, F. P., and Raisaro, J. L. Unifying re-identification, attribute inference, and data reconstruction risks in differential privacy. In *39th Conference on Neural Information Processing Systems (NeurIPS 2025)*, 2025. Affiliations: Lausanne University Hospital, University of Lausanne, Harvard University, Google DeepMind.
- Li, W., Sun, L., Guan, Z., Zhou, X., and Sap, M. 1-2-3 check: Enhancing contextual privacy in LLM via multi-agent reasoning. In Derczynski, L., Novikova, J., and Chen, M. (eds.), *Proceedings of the The First Workshop on LLM Security (LLMSEC)*, pp. 115–128, Vienna, Austria, August 2025. Association for Computational Linguistics. ISBN 979-8-89176-279-4. URL <https://aclanthology.org/2025.llmsec-1.9/>.
- Loshchilov, I. and Hutter, F. Decoupled weight decay regularization. In *Proceedings of the 7th International Conference on Learning Representations (ICLR 2019)*, 2019. Affiliation: University of Freiburg, Germany.
- Mangaokar, N., Hooda, A., Li, Z., Malin, B. A., Fawaz, K., Jha, S., Prakash, A., and Chowdhury, A. R. What really is a member? discrediting membership inference via poisoning. In *39th Conference on Neural Information Processing Systems (NeurIPS 2025)*, 2025. Affiliations: University of Michigan, Ann Arbor; University of Wisconsin-Madison; Vanderbilt University.
- Marreed, S., Oved, A., Yaeli, A., Shlomov, S., Levy, I., Sela, A., Adi, A., and Mashkif, N. Towards enterprise-ready computer using generalist agent. *arXiv preprint arXiv:2503.01861*, 2025. URL <https://arxiv.org/pdf/2503.01861v1>.
- Meeus, M., Shilov, I., Jain, S., Faysse, M., Rei, M., and de Montjoye, Y.-A. Sok: Membership inference attacks on llms are rushing nowhere (and how to fix it). In *2025*

- IEEE Conference on Secure and Trustworthy Machine Learning (SaTML)*, pp. 385–401, Copenhagen, Denmark, 2025. IEEE. doi: 10.1109/SaTML64287.2025.00028.
- Nasr, M., Rando, J., Carlini, N., Hayase, J., Jagielski, M., Cooper, A. F., Ippolito, D., Choquette-Choo, C. A., Tramèr, F., and Lee, K. Scalable extraction of training data from aligned, production language models. In *The Thirteenth International Conference on Learning Representations (ICLR 2025)*, 2025. URL <https://arxiv.org/pdf/2311.17035>.
- Pan, J., Wang, X., Neubig, G., Jaitly, N., Ji, H., Suhr, A., and Zhang, Y. Training software engineering agents and verifiers with swe-gym. In *Proceedings of the 42nd International Conference on Machine Learning (ICML 2025)*, pp. PMLR 267, Vancouver, Canada, 2025. Proceedings of Machine Learning Research.
- Patil, V., Stengel-Eskin, E., and Bansal, M. The sum leaks more than its parts: Compositional privacy risks and mitigations in multi-agent collaboration. *arXiv preprint arXiv:2509.14284*, 2025. URL <https://arxiv.org/pdf/2509.14284>. Affiliations: UNC Chapel Hill, The University of Texas at Austin.
- Prabhakar, A., Liu, Z., Zhu, M., Zhang, J., Awalganekar, T., Wang, S., Liu, Z., Chen, H., Hoang, T., Niebles, J. C., Heinecke, S., Yao, W., Wang, H., Savarese, S., and Xiong, C. Apigen-mt: Agentic pipeline for multi-turn data generation via simulated agent-human interplay. *39th Conference on Neural Information Processing Systems (NeurIPS 2025)*, 2025. Affiliation: Salesforce AI Research, USA.
- Raza, S., Sapkota, R., Karkee, M., and Emmanouilidis, C. Responsible agentic reasoning and ai agents: A critical survey. *TechRxiv preprint*, November 2025. doi: 10.36227/techrxiv.175735299.97215847. URL <https://www.techrxiv.org/doi/full/10.36227/techrxiv.175735299.97215847>. Affiliations: Vector Institute; Cornell University; University of Groningen.
- Rosser, J. and Foerster, J. Agentbreeder: Mitigating the ai safety risks of multi-agent scaffolds via self-improvement. In *39th Conference on Neural Information Processing Systems (NeurIPS 2025)*, 2025. Affiliations: University of Oxford; FLAIR, University of Oxford.
- Shao, Y., Li, T., Shi, W., Liu, Y., and Yang, D. PrivacyLens: Evaluating privacy norm awareness of language models in action. In *38th Conference on Neural Information Processing Systems (NeurIPS 2024), Track on Datasets and Benchmarks*, 2024. Affiliations: Stanford University; Northeastern University; Harvard University.
- Shokri, R., Stronati, M., Song, C., and Shmatikov, V. Membership inference attacks against machine learning models. In *2017 IEEE Symposium on Security and Privacy (SP)*, pp. 3–18. IEEE, 2017.
- Srivastava, S. S. and He, H. Memorygraft: Persistent compromise of llm agents via poisoned experience retrieval. *arXiv preprint arXiv:2512.16962*, 2025. URL <https://arxiv.org/pdf/2512.16962>. Affiliation: School of Computing, University of Georgia, Athens, GA, USA.
- Staab, R., Vero, M., Balunovic, M., and Vechev, M. Large language models are advanced anonymizers. *arXiv preprint arXiv:2402.13846*, 2024. URL <https://arxiv.org/abs/2402.13846>.
- Talebirad, Y. and Nadiri, A. Multi-agent collaboration: Harnessing the power of intelligent llm agents. *arXiv preprint arXiv:2306.03314*, 2023. URL <https://arxiv.org/abs/2306.03314>.
- Wu, G., Zhang, Z., Zhang, Y., Wang, W., Niu, J., Wu, Y., and Zhang, Y. I know what you asked: Prompt leakage via kv-cache sharing in multi-tenant llm serving. In *Network and Distributed System Security (NDSS) Symposium 2025*, San Diego, CA, USA, 2025. doi: 10.14722/ndss.2025.241772. URL <https://dx.doi.org/10.14722/ndss.2025.241772>.
- Xiao, Y., Sun, E., Luo, D., and Wang, W. Tradingagents: Multi-agents llm financial trading framework. In *arXiv preprint arXiv:2412.20138*, 2024. Available at <https://arxiv.org/abs/2412.20138>.
- Xu, Y., Bosselut, A., and Schlag, I. Positional fragility in llms: How offset effects reshape our understanding of memorization risks. In *Proceedings of the 39th Conference on Neural Information Processing Systems (NeurIPS 2025)*, ETH Zürich, 2025. NeurIPS.
- Yang, Y., Chai, H., Shao, S., Song, Y., Qi, S., Rui, R., and Zhang, W. Agentnet: Decentralized evolutionary coordination for llm-based multi-agent systems. In *39th Conference on Neural Information Processing Systems (NeurIPS 2025)*, 2025. Affiliations: Shanghai Jiao Tong University; Shanghai Innovation Institute.
- Zhang, Q., Sun, Y., Jin, C., Zhang, X., Shu, Y., Zhao, P., Shen, L., and Tao, D. Effective policy learning for multi-agent online coordination beyond submodular objectives. In *39th Conference on Neural Information Processing Systems (NeurIPS 2025)*, 2025. Affiliations: Nanyang Technological University, Singapore; The University of Sydney; Hong Kong University of Science and Technology (Guangzhou); Rutgers University; Sun Yat-sen University.

Zhang, Y. and Yang, D. Searching for privacy risks in llm agents via simulation. *arXiv preprint arXiv:2508.10880*, 2025. URL <https://arxiv.org/abs/2508.10880>.

A. Appendix

A.1. Proof of Theorem 4.1

We provide the full derivation of the cumulative leakage bound stated in Theorem 4.1. The proof relies on repeated applications of the chain rule for mutual information (MI) and the conditional data processing inequality as given below.

Model Setup. We consider the sequential multi-agent system defined in Section 3.1 and briefly recall the notation and assumptions required for the theoretical analysis.

Let S_i denote the agent-local sensitive variable accessible only to agent a_i , O_i the intermediate output produced by agent a_i , and D_i the task-relevant or public input available at stage i . Agent outputs satisfy the update rule $O_i = A_i(O_{i-1}, D_i, S_i)$, with $O_0 = \emptyset$.

We assume that the sensitive variables $\{S_i\}_{i=1}^N$ are mutually independent and that the sequential pipeline satisfies the conditional Markov structure defined in Eq. (2). Finally, each agent satisfies a local information leakage constraint as

$$I(O_i; S_i) \leq \epsilon_i. \quad (13)$$

Objective. Our goal is to upper bound the total compositional leakage:

$$I(O_N; S_1, \dots, S_N), \quad (14)$$

in terms of the per-agent leakage budgets $\{\epsilon_i\}_{i=1}^N$.

Chain Rule Expansion. By the chain rule for MI:

$$I(O_N; S_1, \dots, S_N) = \sum_{i=1}^N I(O_N; S_i | S_{<i}). \quad (15)$$

Conditional Data Processing.

Definition A.1 (Conditional Data Processing Inequality). If $X \rightarrow Y \rightarrow Z$ forms a Markov chain conditioned on W , then

$$I(X; Z | W) \leq I(X; Y | W).$$

Applying Definition A.1 to the conditional Markov chain in Eq. (2), we obtain:

$$I(O_N; S_i | S_{<i}) \leq I(O_i; S_i | S_{<i}). \quad (16)$$

Substituting into Eq. (15) yields:

$$I(O_N; S_1, \dots, S_N) \leq \sum_{i=1}^N I(O_i; S_i | S_{<i}). \quad (17)$$

Conditional Leakage Decomposition. We define:

$$\mathcal{L}_i := I(O_i; S_i | S_{<i}). \quad (18)$$

Since S_i is independent of $S_{<i}$, we have:

$$\begin{aligned} \mathcal{L}_i &= H(S_i | S_{<i}) - H(S_i | O_i, S_{<i}) \\ &= H(S_i) - H(S_i | O_i, S_{<i}). \end{aligned} \quad (19)$$

Similarly,

$$I(O_i; S_i) = H(S_i) - H(S_i | O_i). \quad (20)$$

Subtracting the two expressions yields:

$$\begin{aligned} \mathcal{L}_i - I(O_i; S_i) &= H(S_i | O_i) - H(S_i | O_i, S_{<i}) \\ &= I(S_i; S_{<i} | O_i). \end{aligned} \quad (21)$$

Therefore,

$$\mathcal{L}_i = I(O_i; S_i) + I(S_i; S_{<i} | O_i). \quad (22)$$

Bounding Cross-Dependencies.

Lemma A.2 (Upstream Leakage Bound). *For each i , the following inequality holds:*

$$I(S_i; S_{<i} | O_i) \leq I(S_{<i}; O_{i-1}).$$

Proof. Since S_i is independent of $S_{<i}$, we have:

$$I(S_i; S_{<i} | O_i) = I(S_{<i}; O_i | S_i) - I(S_{<i}; O_i).$$

The second term is non-negative, yielding:

$$I(S_i; S_{<i} | O_i) \leq I(S_{<i}; O_i | S_i).$$

By the conditional Markov structure $S_{<i} \rightarrow O_{i-1} \rightarrow O_i$ given S_i , the data processing inequality implies:

$$I(S_{<i}; O_i | S_i) \leq I(S_{<i}; O_{i-1} | S_i) = I(S_{<i}; O_{i-1}),$$

where the final equality follows from independence. \square

Recursive Inequality. By Lemma A.2 and Eq. (22):

$$\mathcal{L}_i \leq I(O_i; S_i) + I(S_{<i}; O_{i-1}). \quad (23)$$

Using the chain rule:

$$I(S_{<i}; O_{i-1}) = \sum_{j=1}^{i-1} I(S_j; O_{i-1} | S_{<j}). \quad (24)$$

Applying conditional data processing again:

$$I(S_j; O_{i-1} | S_{<j}) \leq I(S_j; O_j | S_{<j}) = \mathcal{L}_j.$$

Thus,

$$\mathcal{L}_i \leq \epsilon_i + \sum_{j=1}^{i-1} \mathcal{L}_j. \quad (25)$$

Solving the Recurrence. Define $U_k := \sum_{j=1}^k \mathcal{L}_j$. From Eqs. (17) and (18), we note that

$$I(O_N; S_1, \dots, S_N) \leq U_N. \quad (26)$$

From Eq. (25), we have:

$$U_i = U_{i-1} + \mathcal{L}_i \leq \epsilon_i + 2U_{i-1}.$$

Solving recursively yields:

$$\begin{aligned} U_1 &\leq \epsilon_1 \\ U_2 &\leq \epsilon_2 + 2\epsilon_1 \\ U_3 &\leq \epsilon_3 + 2\epsilon_2 + 4\epsilon_1 \\ &\vdots \\ U_N &\leq \sum_{i=1}^N 2^{N-i} \epsilon_i. \end{aligned} \quad (27)$$

Conclusion. From Eq. (26), we obtain:

$$I(O_N; S_1, \dots, S_N) \leq \sum_{i=1}^N 2^{N-i} \epsilon_i \quad (28)$$

In the uniform case $\epsilon_i = \epsilon$:

$$I(O_N; S_1, \dots, S_N) \leq (2^N - 1)\epsilon.$$

A.2. Experimental Setup Details

A.2.1. TASKS AND DATASETS

MedQA (Medical Reasoning). We use the English subset of MedQA (Jin et al., 2020), consisting of multiple-choice clinical questions that require multi-step medical reasoning. MedQA reflects high-stakes healthcare workflows, where intermediate reasoning states may encode sensitive clinical attributes, implicit diagnoses, or proprietary decision logic.

FinQA (Financial Reasoning). FinQA (Chen et al., 2021) is a financial question-answering benchmark grounded in real-world corporate reports. The task requires numerical reasoning over tabular and textual evidence, making it a privacy-sensitive setting where intermediate representations may encode confidential financial indicators or internal analytical strategies.

PrivacyLens (Contextual Privacy Norms). PrivacyLens (Shao et al., 2024) evaluates privacy norm compliance in action-based agent workflows. Each data point is constructed hierarchically from a privacy-sensitive seed (encoded as a five-tuple specifying data type, data subject, sender, recipient, and transmission principle), which is expanded into a natural-language vignette and an executable agent trajectory. The trajectory consists of a sequence of agent actions and environment observations that simulate a privacy-critical scenario, excluding the final action.

In our experiments, agents consume the seed, vignette, and observed trajectory and must generate the final action. PrivacyLens evaluates whether this action leaks sensitive information specified in the seed while maintaining task helpfulness, enabling realistic assessment of sequential privacy leakage.

A.2.2. SEQUENTIAL AGENT ARCHITECTURES

We evaluate sequential pipelines with $N \in \{2, 3, 4, 5\}$ agents. Each agent is an independent LLM with no shared parameters and communicates exclusively through intermediate representations produced by upstream agents.

The agent roles are instantiated as follows:

- **Agent a_1 (Input Interpreter):** processes the user input (question or trajectory context) and produces an initial structured representation.
- **Agent a_2 (Task Reasoner):** consumes upstream representations and performs core task-level reasoning or decision-making.
- **Agent a_3 (Context Refiner, when $N \geq 3$):** refines and contextualizes intermediate outputs, potentially aggregating partial evidence or reformulating reasoning traces.
- **Agent a_4 (Privacy-Aware Rewriter, when $N \geq 4$):** performs representation-level rewriting or filtering to reduce leakage of agent-local sensitive information while preserving task utility.
- **Agent a_5 (Compliance Checker, when $N = 5$):** performs a final consistency and safety pass, ensuring that the output satisfies both task correctness and privacy constraints before release.

This design reflects realistic multi-agent deployments, where interpretation, reasoning, refinement, and policy enforcement are handled by specialized components operating sequentially. Importantly, increasing agent depth introduces additional opportunities for compositional information leakage, making this setting well-suited for studying privacy amplification effects.

A.2.3. MODELS

We evaluate two open-weight model families:

- **Qwen²:** 2B and 4B parameter variants
- **LLaMA³:** 3B and 7B parameter variants

All agents are fine-tuned using LoRA (Hu et al., 2021) adapters with rank 8. Unless stated otherwise, agents do not share LoRA parameters.

²<https://huggingface.co/Qwen/Qwen2-1.5B>, <https://huggingface.co/Qwen/Qwen1.5-4B-Chat>

³<https://huggingface.co/meta-llama/Llama-3.2-3B>, <https://huggingface.co/meta-llama/Llama-2-7b>

A.2.4. SENSITIVE VARIABLES

Each agent a_i is associated with an agent-local sensitive variable S_i , which should not be inferable from its output O_i .

- For MedQA and FinQA, S_i includes embeddings of private prompts, internal routing states, or agent-specific policy indicators.
- For PrivacyLens, S_i corresponds to privacy-sensitive seed elements, including data subject, recipient, and transmission principle.

A.2.5. TRAINING OBJECTIVE

The privacy-regularized objective is

$$\mathcal{L}_{\text{total}} = \mathcal{L}_{\text{utility}} + \sum_{i=1}^N \beta_i \hat{I}_{\text{MINE}}(O_i; S_i),$$

where $\hat{I}_{\text{MINE}}(O_i; S_i)$ is estimated using stabilized variational MI estimator (MINE). (Belghazi et al., 2018) Privacy weights β_i control the privacy-utility trade-off and are ablated in Appendix A.5.

A.2.6. IMPLEMENTATION DETAILS

All models are trained using AdamW (Loshchilov & Hutter, 2019) with learning rate 2×10^{-5} and batch size 16. MI critics are two-layer MLPs with hidden dimension 256 and ReLU activations. All experiments are run with three random seeds and results are averaged.

A.3. Detailed Evaluation Metrics

This section provides formal definitions and implementation details for all privacy and utility metrics used throughout the paper. Our metrics are designed to jointly capture representation-level information leakage, adversarial inference success, and task utility in sequential multi-agent pipelines.

A.3.1. UTILITY METRICS

Cross-Entropy Loss (CE). For MedQA and FinQA, utility is primarily measured using the standard CE loss between the model prediction \hat{y} and the ground-truth label y , where x denotes the input query and $p_\theta(\cdot | x)$ is the predictive distribution of the final agent parameterized by θ :

$$\text{CE} = -\mathbb{E}_{(x,y)} [\log p_\theta(\hat{y} = y | x)].$$

Lower values indicate better task performance.

Benign Succeeded (BS). BS measures the fraction of benign (non-sensitive) inputs for which the system produces a correct or helpful output, where N_{benign} denotes the number of benign evaluation instances and $\mathbb{I}[\cdot]$ is the indicator function:

$$\text{BS} = \frac{1}{N_{\text{benign}}} \sum_{i=1}^{N_{\text{benign}}} \mathbb{I}[\hat{y}_i = y_i].$$

For PrivacyLens, $\hat{y}_i = y_i$ is replaced by a helpfulness score ≥ 2 on the 0-3 rubric provided by the benchmark. Higher values are better.

A.3.2. REPRESENTATION-LEVEL PRIVACY METRICS

Estimated Mutual Information. For each agent a_i , we estimate the MI between its output representation O_i and its agent-local sensitive variable S_i , where O_i denotes the intermediate representation produced by agent a_i and S_i denotes the corresponding sensitive attribute accessible only at that stage:

$$\hat{I}_{\text{MINE}}(O_i; S_i).$$

MI is estimated using variational MI estimators (MINE) (Belghazi et al., 2018). Lower MI indicates weaker statistical dependence and stronger privacy protection.

Average Mutual Information. To summarize privacy leakage across the depth of a sequential pipeline, we report the average MI

$$\text{MI}_{\text{avg}} = \frac{1}{N} \sum_{i=1}^N \hat{I}_{\text{MINE}}(O_i; S_i),$$

where N denotes the number of agents in the pipeline and $\hat{I}_{\text{MINE}}(O_i; S_i)$ is the estimated MI at agent a_i .

A.3.3. ADVERSARIAL PRIVACY METRICS

Leakage Accuracy (LA). LA measures the success rate of an adversary \mathcal{A} that attempts to infer sensitive attributes from agent outputs. Let O_i denote the output representation produced by agent a_i , S_i the corresponding ground-truth sensitive attribute, and $\hat{S}_i = \mathcal{A}(O_i)$ the adversary’s prediction obtained by applying \mathcal{A} to the agent output:

$$\text{LA} = \frac{1}{N_{\text{sensitive}}} \sum_{i=1}^{N_{\text{sensitive}}} \mathbb{I}[\hat{S}_i = S_i],$$

where $N_{\text{sensitive}}$ denotes the number of sensitive evaluation instances and $\mathbb{I}[\cdot]$ is the indicator function. Lower values indicate stronger privacy protection.

Sensitive Blocked (SB). SB measures the fraction of sensitive cases in which the adversary fails to correctly infer the sensitive attribute:

$$\text{SB} = \frac{1}{N_{\text{sensitive}}} \sum_{i=1}^{N_{\text{sensitive}}} \mathbb{I}[\hat{S}_i \neq S_i] = 1 - \text{LA}.$$

Higher values indicate stronger resistance to adversarial inference.

A.3.4. JOINT PRIVACY-UTILITY METRICS

Balanced Outcome (BO). BO summarizes the privacy-utility trade-off by averaging benign success and sensitive blocking:

$$\text{BO} = \frac{1}{2}(\text{BS} + \text{SB}).$$

This metric penalizes methods that optimize privacy at the expense of utility, or vice versa, by assigning equal weight to both objectives.

Overall Success (OS). OS measures whether a system simultaneously succeeds on benign inputs and blocks sensitive leakage. For paired benign/sensitive evaluation scenarios, let N_{pairs} denote the number of paired instances, $\text{BenignCorrect}_i \in \{0, 1\}$ indicate whether the benign instance is answered correctly, and $\text{Leakage}_i \in \{0, 1\}$ indicate whether sensitive information is leaked:

$$\text{OS} = \frac{1}{N_{\text{pairs}}} \sum_{i=1}^{N_{\text{pairs}}} \mathbb{I}[\text{BenignCorrect}_i = 1 \wedge \text{Leakage}_i = 0].$$

When paired evaluation is unavailable, we approximate OS as

$$\text{OS} \approx \text{BS} \cdot \text{SB},$$

which assumes independence between benign correctness and leakage events.

A.3.5. PRIVACYLENS-SPECIFIC METRIC MAPPING

PrivacyLens evaluates action-based privacy leakage using Leakage Rate (LR) and Adjusted Leakage Rate (LRh), computed over actions with positive helpfulness. We map these quantities to our metrics as follows:

- **Leakage Accuracy (LA)** := LRh
- **Sensitive Blocked (SB)** := $1 - \text{LRh}$
- **Benign Succeeded (BS)** := fraction of actions with helpfulness ≥ 2
- **Overall Success (OS)** := $\text{BS} \cdot \text{SB}$

This mapping allows consistent comparison between representation-level MI metrics and action-based privacy outcomes.

A.3.6. COMPOSITE METRIC: PRIVACY-AWARE REASONING INDEX (PARI)

To summarize privacy–utility trade-offs in a single scalar metric, analogous to the Responsible Reasoning Index (RRI) introduced by Raza et al. (2025), we define the *Privacy-Aware Reasoning Index (PARI)* as:

$$\text{PARI} = w_1 \cdot \text{RC} + w_2 \cdot \text{OT} + w_3 \cdot \text{PI} + w_4 \cdot \text{RT}.$$

PARI is intended as a system-level summary metric that aggregates multiple existing privacy and utility signals, rather than introducing new primitive measurements.

Reasoning Correctness (RC). We define reasoning correctness directly in terms of benign task success using the Benign Succeeded (BS) metric introduced earlier:

$$\text{RC} := \text{BS}.$$

This choice avoids introducing a separate correctness score and ensures direct consistency between task-level utility evaluation and the composite metric.

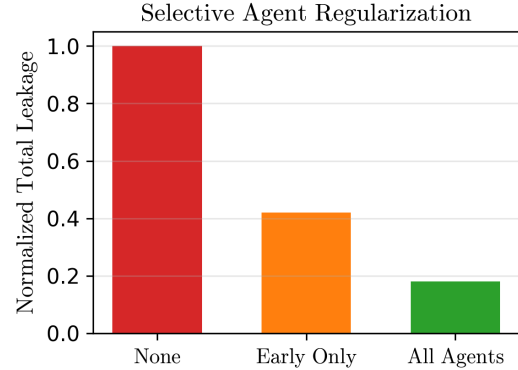


Figure 4. Total compositional leakage under selective agent regularization.

Operational Transparency (OT). Operational Transparency measures the stability of intermediate representations under benign input perturbations. Let q denote a benign input query, $q + \epsilon$ a semantically equivalent perturbation, and $O(\cdot)$ the final system representation produced by the agent pipeline. We define:

$$\text{OT} := 1 - \mathbb{E}[\|O(q) - O(q + \epsilon)\|_2].$$

In our experiments, representation stability remains consistent across methods; thus, OT is treated as constant and does not affect relative comparisons.

Privacy Integrity (PI). Privacy Integrity quantifies the relative reduction in representation-level leakage. Let MI_{avg} denote the average estimated MI across agents for a given method, and $\text{MI}_{\text{baseline}}$ the corresponding value for the unregularized baseline. We define:

$$\text{PI} := 1 - \frac{\text{MI}_{\text{avg}}}{\text{MI}_{\text{baseline}}}.$$

Reproducibility and Traceability (RT). Reproducibility and Traceability capture whether system execution is deterministic and auditable. Since all experiments enforce fixed routing, deterministic decoding, and comprehensive logging, this component is fixed:

$$\text{RT} := 1.$$

Interpretation and Metric Mapping. PARI does not introduce new evaluation primitives; rather, it aggregates previously defined metrics into a single scalar score. Specifically, RC corresponds directly to BS, PI is a normalized function of average representation-level MI, OT captures representation stability under benign perturbations, and RT encodes deterministic execution. This decomposition allows PARI to summarize the privacy–utility trade-off while preserving interpretability in terms of underlying metrics.

Weights. Unless otherwise stated, we use:

$$(w_1, w_2, w_3, w_4) = (0.3, 0.1, 0.5, 0.1),$$

reflecting the central importance of privacy integrity in our evaluation.

A.4. Additional Experiments on PrivacyLens

We provide additional validation of our framework on the **PrivacyLens** benchmark (Shao et al., 2024), which is specifically designed to evaluate privacy leakage and adversarial inference risks in language models. Unlike MedQA and FinQA, PrivacyLens does not emphasize task-level reasoning, but instead probes the model’s ability to resist sensitive attribute inference under controlled adversarial settings.

To isolate privacy behavior in resource-constrained regimes, we report results only for **Qwen-2B** and **LLaMA-3B**. All evaluation metrics follow the same definitions as in Appendix A.3, and all MI estimates are computed using frozen estimators.

A.4.1. PRIVACYLENS RESULTS

Discussion. The PrivacyLens results reinforce the core findings of the main paper. Across both Qwen-2B and LLaMA-3B, MI-regularized training reduces MI_{avg} by approximately **65–80%** relative to unregularized baselines, leading to substantial improvements in resistance to sensitive attribute inference. SB increases consistently across agent depths, while LA decreases in near-linear correspondence with MI_{avg} .

As expected, absolute benign performance (BS) is slightly lower than in MedQA and FinQA, reflecting the adversarial nature of PrivacyLens. Nevertheless, utility degradation remains moderate, and the resulting OS improves by more than an order of magnitude in most settings. These results confirm that the benefits of MI-regularization extend beyond task-centric benchmarks to dedicated privacy stress tests.

Importantly, the observed trends mirror those in the main results: unregularized systems exhibit rapid leakage amplification with agent depth, while MI-regularization effectively suppresses cumulative leakage. This consistency across benchmarks strengthens the case for MI as a principled, system-level control mechanism for privacy in sequential multi-agent LLM deployments.

A.5. Ablation Studies

We conduct a series of ablation studies to analyze the behavior of the proposed privacy-regularized training framework and to validate key design choices. Unless otherwise stated, all ablations are evaluated using validation accuracy as the utility metric and estimated MI leakage $\hat{I}_{MINE}(O_i; S_i)$ as the privacy metric.

A.5.1. EFFECT OF PRIVACY WEIGHT β

We first examine the effect of the privacy regularization strength by sweeping $\beta \in \{0, 10^{-3}, 10^{-2}, 10^{-1}, 1\}$ with

Table 5. PrivacyLens results for lightweight models (B = Baseline, M = MINE-Reg).

Model	Ag	Meth	$MI_{avg} \downarrow$	LA \downarrow	SB \uparrow	BS \uparrow	OS \uparrow	PARI \uparrow
Qwen-2B	2	B	0.64	0.61	0.39	0.90	0.12	0.468
Qwen-2B	2	M	0.12	0.25	0.75	0.86	0.65	0.862
Qwen-2B	3	B	0.82	0.68	0.32	0.87	0.07	0.459
Qwen-2B	3	M	0.17	0.29	0.71	0.80	0.57	0.846
Qwen-2B	4	B	0.98	0.73	0.27	0.84	0.04	0.451
Qwen-2B	4	M	0.22	0.34	0.66	0.77	0.51	0.832
LLaMA-3B	2	B	0.69	0.66	0.34	0.86	0.10	0.453
LLaMA-3B	2	M	0.21	0.37	0.63	0.78	0.49	0.781
LLaMA-3B	3	B	0.87	0.71	0.29	0.83	0.06	0.444
LLaMA-3B	3	M	0.26	0.41	0.59	0.75	0.44	0.776
LLaMA-3B	4	B	1.02	0.75	0.25	0.80	0.04	0.435
LLaMA-3B	4	M	0.31	0.45	0.55	0.72	0.40	0.764

uniform allocation $\beta_1 = \beta_2 = \beta$. This experiment isolates the role of β as a global control parameter governing the privacy-utility trade-off.

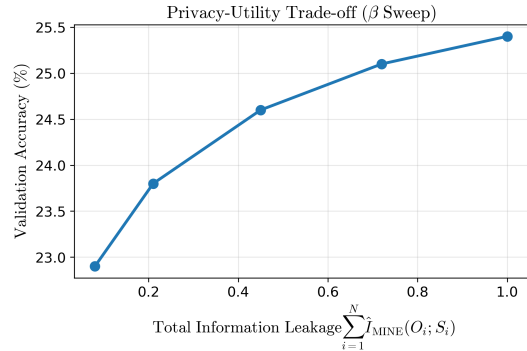


Figure 5. Privacy-utility trade-off as a function of the privacy weight β , measured by validation accuracy versus total information leakage $\sum_{i=1}^N \hat{I}_{MINE}(O_i; S_i)$, for $N=3$ sequential-agent pipeline using Qwen-2B evaluated on MedQA.

Figure 5 reveals a smooth and monotonic trade-off between privacy and utility. As β increases, total information leakage decreases consistently, while validation accuracy degrades gradually rather than catastrophically. Notably, the utility curve exhibits diminishing sensitivity beyond moderate leakage reductions, indicating that a substantial fraction of sensitive information can be removed before task-relevant performance is severely affected.

This behavior suggests that β functions as a stable and interpretable privacy knob, enabling practitioners to select operating points that achieve meaningful privacy gains without incurring abrupt performance collapse. The absence of sharp phase transitions further indicates that the optimization landscape remains well-conditioned across a wide range of privacy budgets.

A.5.2. SELECTIVE AGENT REGULARIZATION

We study whether privacy regularization must be applied to all agents or only to a subset of the pipeline. We compare three settings: (i) no agents regularized, (ii) only early agents regularized, and (iii) all agents regularized. All set-

tings use the same total privacy budget.

Figure 4 shows that regularizing only early agents substantially reduces total leakage relative to the unregularized baseline, highlighting the importance of controlling information release at early stages. However, significant residual leakage persists due to amplification in later agents that remain unconstrained.

Full regularization across all agents consistently achieves the lowest leakage, demonstrating that privacy risks are distributed throughout the pipeline rather than localized to initial stages. This result emphasizes the need for system-level privacy control and cautions against partial defenses that leave downstream agents unregulated.

A.5.3. REPRESENTATION COMPRESSION EFFECTS

We analyze how MI regularization affects the information content of intermediate representations. Specifically, we measure $I(O_i; y)$ (task relevance) and $I(O_i; S_i)$ (privacy leakage) as β increases.

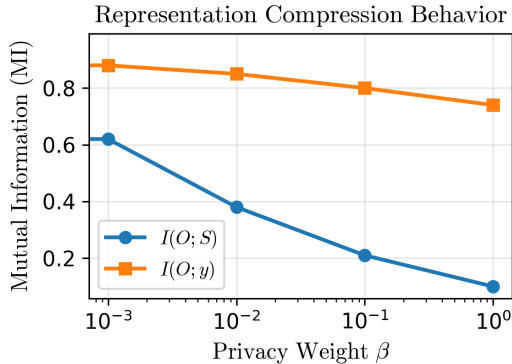


Figure 6. Effect of privacy regularization on task-relevant and sensitive information in intermediate representations.

Figure 6 illustrates that increasing β leads to a pronounced reduction in $I(O_i; S_i)$, while $I(O_i; y)$ decreases much more gradually. This asymmetric compression indicates that the regularizer preferentially suppresses sensitive information rather than indiscriminately collapsing representations.

The preservation of task-relevant signal explains the smooth utility degradation observed in earlier experiments and suggests that the model learns to discard privacy-sensitive features while retaining predictive structure. This behavior aligns with the intended role of information-theoretic regularization as a selective bottleneck rather than a blunt constraint.

A.5.4. ROBUSTNESS TO ADVERSARIAL INFERENCE

Finally, we evaluate whether reductions in MI translate into practical robustness against inference attacks. We train a lightweight adversarial probe to predict the sensitive attribute S_i from agent outputs O_i under varying privacy budgets.

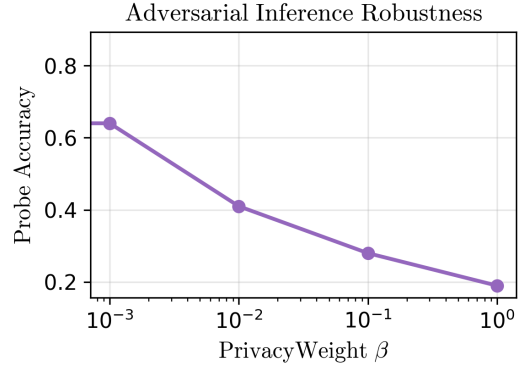


Figure 7. Adversarial probe accuracy for predicting sensitive variables from agent outputs.

As shown in Figure 7, adversarial probe accuracy decreases monotonically as β increases, closely tracking the reduction in estimated MI. At higher privacy weights, probe performance approaches chance level, indicating that sensitive attributes are no longer reliably recoverable from intermediate representations.

This result confirms that MI regularization yields operational privacy benefits beyond metric-level improvements, directly limiting the ability of downstream attackers to exploit latent representations for sensitive inference.

A.6. Extended Related Work

A.6.1. MEMORIZATION AND TRAINING-DATA PRIVACY

Early work on LLM privacy focused on memorization-based risks, demonstrating that models can reproduce rare or repeated training examples verbatim (Xu et al., 2025; Nasr et al., 2025). Membership inference attacks further show that adversaries can determine whether a specific record was used during training (Shokri et al., 2017). Subsequent work explores mitigating these risks using differential privacy during training (Li et al., 2025; Kulynych et al., 2025). While these methods provide strong record-level guarantees, they operate at training time and do not address inference-time leakage arising from contextual reasoning or interaction history.

A.6.2. INFERENCE-TIME PRIVACY AND USER PROFILING

Beyond memorization, inference-time privacy attacks infer sensitive attributes such as demographics, preferences, or intentions from user prompts (Patil et al., 2025; Zhang et al., 2025). User profiling literature similarly studies attribute inference from text (Yang et al., 2025; Gomaa et al., 2025). These attacks typically assume a single model interacting with a single user, and do not capture risks that emerge when partial information is distributed across multiple agents.

A.6.3. CONTEXTUAL INTEGRITY AND PRIVACY NORMS

Contextual integrity theory posits that privacy violations arise when information flows deviate from social norms

defined by actors, information type, and transmission principles (Gomaa et al., 2025; Rosser & Foerster, 2025). Recent work applies this framework to LLMs, emphasizing norm-aware decision making in dialogue systems. PrivacyLens operationalizes these ideas by constructing privacy-sensitive seeds, vignettes, and trajectories for action-based evaluation (Shao et al., 2024). However, these evaluations focus on final actions and do not quantify how intermediate representations accumulate privacy risk across agent pipelines.

A.6.4. MULTI-AGENT SYSTEMS AND MEMORY RISKS

LLM-based multi-agent systems have gained traction for collaborative reasoning, tool use, and autonomous workflows (Talebirad & Nadiri, 2023; Khan & Asif, 2025). A critical component of these systems is shared or persistent memory, which stores intermediate reasoning traces and observations. Recent work highlights that agent memory can be exploited through poisoning or indirect manipulation, enabling targeted misbehavior without direct access to the memory store (Chen et al., 2024; Srivastava & He, 2025). Other studies show that agent topologies and communication patterns introduce unique vulnerabilities absent in single-agent systems.

Despite these advances, existing defenses largely rely on heuristic filtering, memory sanitization, or access control, and lack formal guarantees against privacy leakage arising from sequential composition. Our work complements this literature by providing a principled, representation-level analysis of privacy leakage and a training-time mitigation strategy that scales with agent depth.